

---

CSIRO PUBLISHING

---

# Australian Journal of Physics

Volume 52, 1999  
© CSIRO Australia 1999



A journal for the publication of  
original research in all branches of physics

**[www.publish.csiro.au/journals/ajp](http://www.publish.csiro.au/journals/ajp)**

All enquiries and manuscripts should be directed to

*Australian Journal of Physics*

**CSIRO PUBLISHING**

PO Box 1139 (150 Oxford St)

Collingwood

Vic. 3066

Australia

Telephone: 61 3 9662 7626

Facsimile: 61 3 9662 7611

Email: [peter.robertson@publish.csiro.au](mailto:peter.robertson@publish.csiro.au)



Published by **CSIRO PUBLISHING**  
for CSIRO Australia and  
the Australian Academy of Science



## Interference and Spin Effects in Relativistic (e, 2e) Collisions\*

Stefan Keller

Institut für Theoretische Physik, Universität Frankfurt,  
Robert Mayer-Straße 8-10, D-60054 Frankfurt, Germany.

### Abstract

The interpretation of the triply differential cross sections for ionisation of inner-shell states of high- $Z$  atoms by relativistic electrons is discussed for the case of coplanar asymmetric scattering geometry. It is demonstrated that both strong-field and relativistic interference effects lead to distinct structures in the experimental data. Elements of a similar analysis of spin asymmetries measured in experiments with transversely polarised electrons are also presented.

### 1. Introduction

The ionisation of the inner shell states of atoms by relativistic electron impact has been the subject of theoretical studies since the early days of quantum mechanics. Already the first of these studies by Møller (1931) and Bethe (1933) identified the key features of this process: due to the short collision times, it can reasonably be described in first order perturbation theory, but the relativistic nature of the interaction between the electrons manifests itself in a significantly larger cross section than predicted by nonrelativistic perturbation theory (for a review of this problem see Moiseiwitsch 1980). As only one more recent and spectacular example of the success of this approach, the experimental total cross section for electron impact ionisation of hydrogen-like uranium has accurately been reproduced by two independent calculations (Moores and Reed 1995; Fontes *et al.* 1995) that essentially evaluated the relativistic first order  $S$ -matrix element formulated by Møller (1931) (and later understood to represent the leading term in the perturbation series of quantum electrodynamics, see e.g. Itzykson and Zuber 1980). The only important modification of this theory used in these calculations was to include the strong nuclear potential to all orders by describing the asymptotic states in terms of exact solutions of the Dirac–Coulomb equation. This so-called relativistic distorted wave Born approximation (rDWBA) (Pindzola and Buie 1988; Butler *et al.* 1988; Pindzola *et al.* 1989) is generally considered to be an adequate approach to the description of electron impact ionisation of inner-shell states.

\* Refereed paper based on a contribution to the Australia–Germany Workshop on Electron Correlations held in Fremantle, Western Australia, on 1–6 October 1998.

In view of these results, one might be inclined to believe that the study of inner-shell ionisation in (e,2e) coincidence experiments could add little to our understanding of the dynamics of quantum systems. It is the purpose of this contribution to show that this is not so. Rather, the very fact that the basic mechanisms driving the measured cross sections are known from the outset, allows us to achieve a detailed understanding of the multitude of structures seen in the measured (e,2e) triply differential cross sections (TDCS). Since the exchange of a single virtual photon between two electrons is the elementary building block of all electron correlation phenomena, this sort of analysis contributes important basic information to the detailed understanding of the dynamics of interacting many-body quantum systems.

The present study begins with a down-to-earth introduction to the rDWBA aimed at exhibiting the physical processes built into this model (Section 2). In this light, Section 3 discusses the interpretation of the various features of the TDCS observed in relativistic (e,2e) experiments in coplanar asymmetric geometry. Section 4 is devoted to a discussion of spin effects in relativistic  $K$  and  $L$  shell ionisation processes.

## 2. Pedagogical Introduction to the rDWBA Model

A consistent description of relativistic scattering experiments requires the formalism of quantum electrodynamics. Within this approach, a first principles derivation of the cross section for (e,2e) processes on a multi-electron target meets considerable conceptual problems, so that only the effective two-electron problem has actually been considered explicitly (Keller *et al.* 1994, 1996a; for further discussion of this problem see Keller 1998). In this approximation, Møller (1931) derived the correct structure of the covariant first order  $S$ -matrix element for electron-electron scattering from a plausibility argument. This approach is well suited to highlight all important features of the rDWBA model without recourse to the vast formalism of quantum field theory.

The starting point of Møller's argument is the observation that the nonrelativistic first order  $S$ -matrix element describing the collision of electrons in initial states 0 and  $b$  leaving them in final states 1 and 2 (for simplicity in the following only the direct term is written and natural units  $\hbar = c = m = 1$  are used),

$$S^{(1)} = \int d^3x \varphi_1^*(\mathbf{x}) \varphi_0(\mathbf{x}) \int d^3y \frac{\varphi_2^*(\mathbf{y}) \varphi_b(\mathbf{y})}{|\mathbf{x} - \mathbf{y}|}, \quad (1)$$

can, using the identity

$$\begin{aligned} \varphi_b^*(\mathbf{x}) \varphi_a(\mathbf{x}) &= \int d^3z \delta^{(3)}(\mathbf{x} - \mathbf{z}) \varphi_b^*(\mathbf{z}) \varphi_a(\mathbf{z}) \\ &= \langle b | \hat{\rho}(\mathbf{x}) | a \rangle \quad := \quad \rho_{ba}, \end{aligned} \quad (2)$$

be cast in the form

$$S^{(1)} = \int d^3x \rho_{10}(\mathbf{x}) \int d^3y \frac{\rho_{2b}(\mathbf{y})}{|\mathbf{x} - \mathbf{y}|}, \quad (3)$$

where  $\rho_{10}$  ( $\rho_{2b}$ ) is the matrix element of the density operator associated with the transition of the projectile (target) electron from state 0 to state 1 ( $b$  to 2). In this form, it is evident that the Born matrix element describes the transition of one electron due to the perturbation caused by the transition of its collision partner:

$$\begin{aligned} S^{(1)} &= \int d^3x \rho_{10}(\mathbf{x}) \cdot \Phi_{2b}(\mathbf{x}) \\ &= \int d^3y \rho_{2b}(\mathbf{y}) \cdot \Phi_{10}(\mathbf{y}); \end{aligned} \quad (4)$$

the Coulomb denominator in equation (1) is the Green function of electrostatics, that mediates the interaction in this stationary formalism.

The cross section for any scattering process must be Lorentz invariant (the reaction probability must be independent of the observer frame), hence the  $S$  matrix must be a Lorentz scalar function of Lorentz covariant quantities. Therefore, Møller suggested replacing  $\rho$  and  $\Phi$  in equation (2) by their four vector generalisations, the four current density  $j^\mu = (\rho, \mathbf{j})$  (with the spatial charge current  $\mathbf{j}$ ) and the four potential  $A^\nu := (\Phi, \mathbf{A})$  (with the vector potential  $\mathbf{A}$ ) to construct the Lorentz scalar

$$S^{(1)} = \int d^4x j_{10}^\mu(x) g_{\mu\nu} A_{2b}^\nu(x), \quad (5)$$

where  $g_{\mu\nu}$  is the space-time metric tensor, and the four potential is defined by the covariant Green function  $D^0(x-y)$  of Maxwell's equations,

$$A_{2b}^\nu(x) = \int d^4y D^0(x-y) j_{2b}^\nu(y). \quad (6)$$

Carrying out the summation over Lorentz indices, this first order  $S$  matrix reads

$$S^{(1)} = \int d^4x \rho_{10}(x) \Phi_{2b}(x), - \int d^4x \mathbf{j}_{10}(x) \cdot \mathbf{A}_{2b}(x) \quad (7)$$

$$= S^{\text{long}} - S^{\text{trans}}. \quad (8)$$

Hence in the relativistic theory, the  $S$  matrix is composed of two terms:  $S^{\text{long}}$  describes ionisation by exchange of a longitudinal photon. In the nonrelativistic limit, this contribution reduces to equation (1). In contrast,  $S^{\text{trans}}$  is of purely relativistic origin. It represents interactions by means of a transverse photon, e.g. the coupling between the spatial transition currents of the active electrons.

Having defined the Møller  $S$  matrix in the form of equation (3), it remains to specify the four currents  $j_{10}^\mu$  and  $j_{2b}^\nu$ . For Dirac fermions, these quantities are given by  $j_{ba}^\mu(\mathbf{x}) = \psi_b^\dagger(\mathbf{x}) \gamma^0 \gamma^\mu \psi_a(\mathbf{x})$ , where the  $\psi$  and  $\gamma$  are Dirac bispinors and matrices, respectively (for all associated technical details see Itzykson and Zuber 1980). The various theoretical models discussed in the literature are thus defined by the ansatzes made for the wave functions  $\psi$ . In particular, the rDWBA  $S$

matrix is obtained by substituting exact numerical solutions of the Dirac equation with an effective static potential describing the atomic nucleus and the screening by the spectator electrons, with appropriate scattering boundary conditions for the continuum states (Keller *et al.* 1994). A relativistic version of the standard first order Born approximation (rFBA) uses plane rather than distorted waves for the projectile states 0 and 1 (Keller *et al.* 1996a).

At this point, the physical processes modelled into the rDWBA and rFBA can be spelled out explicitly:

- (1) Both models are based on the covariant Møller  $S$ -matrix element. Therefore they include all effects of the relativistic nature of the electromagnetic interaction between the two electrons within the respective first order approximation. In particular, they describe the magnetic interaction between the orbital and spin currents of the active electrons, as well as retardation effects.
- (2) The rDWBA uses elastic scattering eigenfunctions to describe all continuum states. The interaction between the incoming and outgoing electrons, and the residual ion (treated as a static charge distribution) is therefore described exactly. In contrast, the rFBA includes these effects only for the final state of the initially bound electron, whereas the projectile is assumed not to interact with the ion.

### 3. Interpretation of Inner Shell (e, 2e) TDCS in Coplanar Asymmetric Geometry

The first rDWBA calculations for relativistic (e, 2e) TDCS were reported in 1994 (Ast *et al.* 1994; Keller *et al.* 1994). As could be expected from the success of the distorted wave Born model for total cross sections (see the Introduction), and for inner shell (e, 2e) processes at nonrelativistic energies (Zhang *et al.* 1992), qualitative and in many cases quantitative agreement with the relative and absolute TDCS measured by W. Nakel and his collaborators in Tübingen was obtained. The present section is devoted to an interpretation of a subset of these experimental data in terms of the physical processes included in the rDWBA. It summarises and extends theoretical results recently reported (Keller and Dreizler 1998; Keller *et al.* 1999; to be referred to as papers I and II respectively).

#### (3a) Analysis of an (e, 2e) Experiment on Copper

In 1997, Besch *et al.* reported on an (e, 2e) experiment with 300 keV electrons on the  $K$  electrons of copper (binding energy  $E_b = 8.979$  keV). The electrons were detected in a coplanar asymmetric geometry (see Fig. 1 which introduces the notation used) at energies of 220 and 71 keV respectively. The TDCS measured shows a number of distinct features (Fig. 2), notably

- a substantial shift of the binary peak away from the direction of momentum transfer towards larger angles. This effect has been observed in all relativistic (e, 2e) experiments (see e.g. Bonfert *et al.* 1991).
- a pronounced secondary maximum for emission of both electrons into the same quadrant. This effect was also manifest in TDCS measured by Bonfert *et al.* (1991) and Prinz *et al.* (1995).
- a secondary peak structure in the recoil regime at  $\theta_2 \sim 95^\circ$ . This type of signature had not been seen in previous (e, 2e) measurements in Ehrhardt geometry.

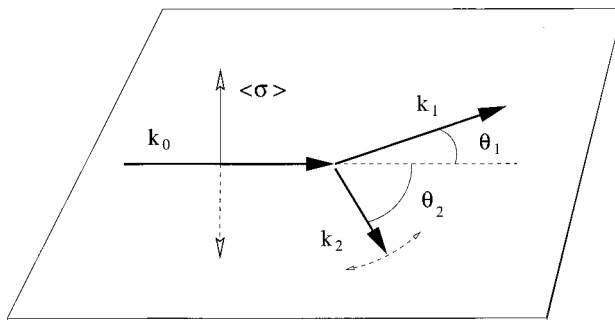


**Fig. 1.** Schematic representation of an  $(e, 2e)$  experiment in coplanar asymmetric unequal energy sharing geometry. The triply differential cross section is measured as function of  $\theta_2$ . The arrows perpendicular to the scattering plane represent the orientations of incident electron spin in experiments with transversely polarised beams.

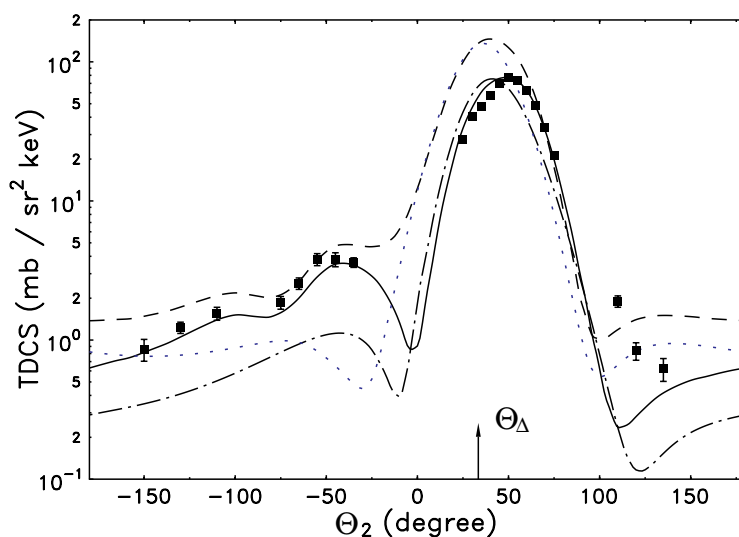


**Fig. 2.** TDCS for  $(e, 2e)$  on the  $1s_{1/2}$  state of copper ( $Z = 29$ ). Impact energy is  $T_0 = 300$  keV, slow outgoing electron energy is  $T_2 = 71$  keV, and fast electron observation angle is  $\theta_1 = -9^\circ$ . Symbols: relative experimental data (Besch *et al.* 1997), normalised to rDWBA calculation at the maximum; full curve: result of rDWBA calculation (Dreizler *et al.* 1997), dashed curve: result of rDWBA calculation including only  $S^{\text{long}}$ , dash-dot curve: result of rFBA calculation, and dotted curve: result of rFBA calculation including only  $S^{\text{long}}$  (Keller and Dreizler 1998). The arrow labelled  $\Theta_\Delta$  indicates the direction of momentum transfer.

Fig. 2 shows that these relative data are quantitatively described by the rDWBA calculation of Dreizler *et al.* (1997). This indicates that an explanation of all the features listed above in terms of consequences of the relativistic nature of the electron–electron interaction and of elastic scattering of the continuum electrons in the spectator ion field should be possible.

The starting point of the detailed analysis of this experiment reported in paper I was the observation that an rFBA calculation qualitatively reproduced

the shift of the binary peak and the occurrence of the secondary maximum, but failed to predict the additional structure in the backward half-plane. From an analysis of the symmetry properties of the rFBA  $S$  matrix (using a simplified analytical version of this quantity to exhibit its characteristic dependencies on the asymptotic momenta) it was concluded in paper I that the features qualitatively predicted by the rFBA are due to the interference of the amplitudes  $S^{\text{long}}$  and  $S^{\text{trans}}$ . Indeed, Fig. 2 shows that upon retaining only  $S^{\text{long}}$  in an rFBA calculation, the symmetry with respect to the direction of momentum transfer is recovered, and the secondary maximum disappears.

The maximum at large angles can only be due to the interaction between the projectile electron and the spectator ion (exchange effects play no role due to the strongly asymmetric energy sharing). In paper I, a perturbative argument introduced by Briggs (1986) was used to show that such a structure can occur as a result of a second-order process in which the electron first scatters off the spectator ion and subsequently ionises the bound electron. The probability for this process has a sharp maximum for the case of zero momentum transfer to the spectator ion during the ionising electron–electron collision (bound electron Bethe ridge condition). From the corresponding kinematical constraints, the position of the secondary peak could be accurately estimated. The numerical calculation shows that this structure is also present in rDWBA-type data obtained using only  $S^{\text{long}}$ , indicating that it is unrelated to the relativistic interference effect discussed above. Furthermore, these data show that projectile rescattering also influences the peak shift (Ast *et al.* 1996) as well as the magnitude of the secondary maximum (see paper I).

### (3b) Spectator Ion Field Effects

The analysis of paper I was based on the fact that the effect of projectile scattering in the external field could be estimated using perturbation theory. FBA-type models fail completely for all Tübingen experiments with gold targets (Keller *et al.* 1996a), indicating that this approach is invalid for systems with high atomic number. It is therefore of interest to study the atomic number dependence of the TDCS in order to identify the signatures of such non-perturbative strong field effects.

As recently discussed in paper II, the comparison of  $(e, 2e)$  data for different targets is complicated by the different binding energies entering into the definition of the respective  $(e, 2e)$  kinematics. The usual expedient of scaling the results to eliminate this influence is not available in relativistic problems due to the presence of the electron rest mass as an invariant energy scale. Therefore, in their very recent experimental study of atomic number dependent effects in  $K$  shell ionisation TDCS, Sauter *et al.* (1998a) resorted to comparing results for the same impact and slow outgoing electron energies. This procedure was subsequently justified in paper II. In the present work, a different point of view is taken. It is based on the fact that the ionisation potentials of the silver  $1s_{1/2}$  state and the uranium  $2p_{3/2}$  are quite similar (25.5 and 17.2 keV respectively). Hence both systems can be studied with essentially the same scattering kinematics, a fact first used in Besch *et al.* (1998) (see Section 4). The main disadvantage of this comparison is the different angular momentum and nodal structure of the

respective bound state one-electron orbitals. However, since this defect is entirely different from the mismatch of the kinematics, this procedure complements the work of (Sauter *et al.* 1998*a*; paper II) because it is very unlikely that artefacts of one method will manifest themselves in the other approach as well.

Fig. 3 shows calculated results for these two targets. Following Sauter *et al.* (1998*a*), impact and slow outgoing electron energy as well as fast electron scattering angle were chosen as in the copper data of Fig. 2. This also allows a comparison with the experimental data of Sauter *et al.* (1998*a*) for the silver  $1s_{1/2}$  state. The results for silver are remarkably similar to the copper ones, indicating

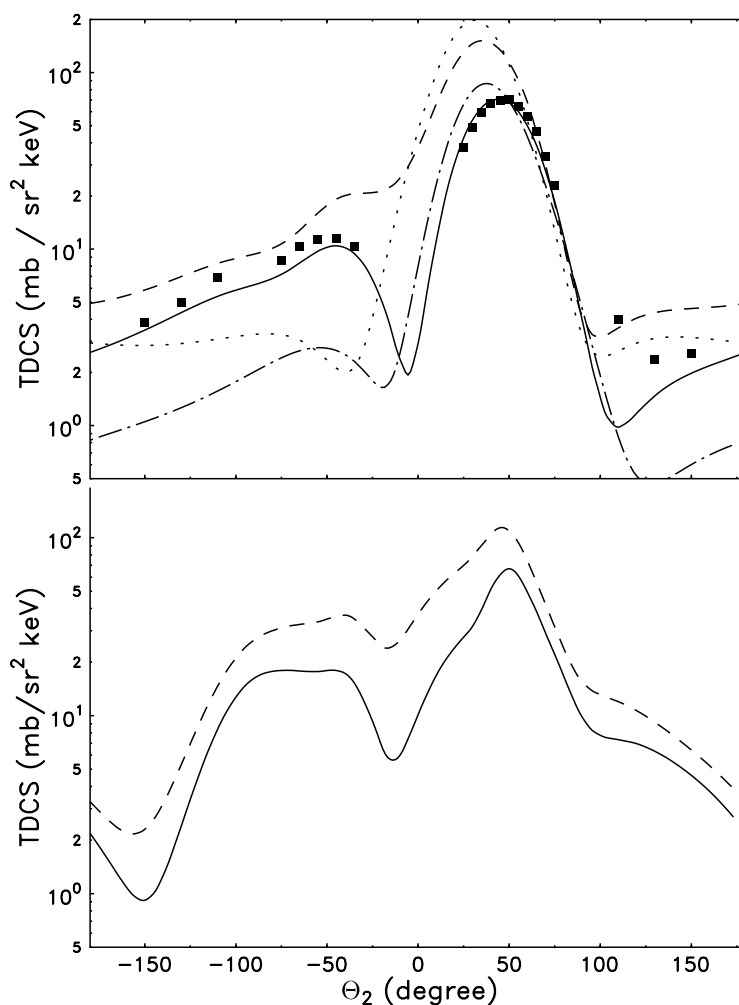


**Fig. 3.** TDCS for (e,2e) on inner shell states of silver ( $Z = 47$ ) and uranium ( $Z = 92$ ). Impact energy is  $T_0 = 300$  keV, slow outgoing electron energy  $T_2 = 71$  keV, and fast electron observation angle  $\theta_1 = -9^\circ$ . Full curve: result of rDWBA calculation, dashed curve: result of rDWBA calculation including only  $S^{\text{long}}$ . *Top*: Results for silver  $1s_{1/2}$  shell; symbols: relative experimental data (Sauter *et al.* 1998*a*), dash-dot curve: rFBA calculation, and dotted curve: result of rFBA calculation including only  $S^{\text{long}}$ . *Bottom*: Results for uranium  $2p_{3/2}$  shell.



that the basic physical mechanisms discussed above can also be invoked to explain this experiment. However, the data also show that a non-perturbative treatment of the projectile-spectator ion interaction is more important in the silver case: the rFBA approach fails to reproduce the absolute magnitude of the rDWBA TDCS even in the binary region (in contrast to the case of copper); moreover, the calculated double scattering signature is significantly less pronounced. The rDWBA calculation slightly underestimates the measured relative magnitude of the TDCS in the recoil regime.

The differences between the silver and uranium results are dramatic: the secondary maximum changes for uranium is plateau- rather than peak-shaped. Of course, this effect might in part be due to the different bound state structure [note that the ‘deformed’ shape of the binary peak is due to the presence of a minimum of the TDCS at the bound electron Bethe ridge point in  $p$  state ionisation (Kull *et al.* 1997)]. However, the same characteristic shape of the TDCS for negative  $\theta_2$  has also been predicted for  $K$  shell (e,2e) at high atomic number (Keller *et al.* 1994), and has indeed recently been observed by Sauter *et al.* (1998a) in their experiment on the gold  $1s_{1/2}$  state. As was shown in paper II, the flattening of the cross section in the recoil regime is associated with a particularly strong influence of  $S^{\text{trans}}$ . In the present uranium results, this effect is weaker, and also somewhat disguised by the logarithmic representation (notice the change of slope at  $-80^\circ < \theta_2 < -40^\circ$ ).

#### 4. Spin Phenomena in Relativistic (e,2e) Physics

The results of papers I and II, and of the previous section, show that all structures of the TDCS observed in coplanar asymmetric geometry could be associated with the physical processes included in the rDWBA model description. The (e,2e) experiments with polarised beams represent a further step towards the ideal of a quantum mechanically complete experiment, so that it is natural to search for a similar detailed interpretation of the additional spin-dependent observables.

To date, the understanding of spin phenomena in (e,2e) experiments is not as advanced as that of the TDCS. Therefore in this section, the individual spin sensitive processes, that could manifest themselves in relativistic (e,2e) experiments, will be discussed separately. Where possible, experimental signatures of these phenomena will be identified.

##### (4a) Exchange Scattering

The most obvious spin effect in electron–electron scattering is due to the Pauli principle: even in a free binary Coulomb collision, the Pauli principle requires the coordinate space wave function of the singlet (triplet) state to be symmetric (antisymmetric), so that the respective cross sections differ in the sign of the term due to interference between direct and exchange scattering amplitudes. In particular, triplet scattering has zero cross section if the final state is symmetric under interchange of all observed quantum numbers. In an (e,2e) experiment, this effect may manifest itself in a minimum of the cross section for the case of symmetric equal energy sharing geometry even if the spin degrees of freedom are not observed.

One suitable geometry for observing this effect is an arrangement in which both electrons are observed in the scattering plane with the same energy and under a fixed relative angle  $\Theta_{1,2}$ , and the TDCS is recorded as function of the relative angle of the axis of symmetry of this arrangement with the beam axis (Whelan *et al.* 1996). It should be emphasised that the ‘Pauli blocking’ effect, in this reference discussed for relativistic (e, 2e) processes in the context of the rDWBA, is neither of relativistic nor strong-field origin, but already features in the nonrelativistic plane wave impulse approximation.

#### (4b) Continuum Spin–Orbit Coupling

The basic mechanism of spin–orbit coupling in the continuum is well known from elastic (Mott) scattering of transversely polarised high-energy electrons. A pictorial interpretation of the resulting spin asymmetry

$$A := \frac{d\sigma(\uparrow) - d\sigma(\downarrow)}{d\sigma(\uparrow) + d\sigma(\downarrow)} \quad (9)$$

has been given by Kessler (1985). From the important influence of elastic scattering of the continuum electrons on the TDCS discussed in Section 3, it is evident that a corresponding spin asymmetry might also occur in relativistic (e, 2e) processes even for *s* state ionisation (Prinz *et al.* 1995), where in the nonrelativistic energy regime this quantity is strictly zero provided that LS coupling is applicable (Keller *et al.* 1996*b*).

Prinz *et al.* (1995) argued that because electron–nucleus interactions play a subordinate role in the scattering kinematics of the binary peak, the asymmetry values should be very small in this regime. In contrast, for emission of both electrons into the same half-plane, the spectator ion has to balance their transverse momentum, so that these interactions must be strong, hence larger spin–orbit coupling effects should be seen. This expectation was confirmed by experiment (Prinz *et al.* 1995; Prinz and Keller 1996). Subsequently it was noticed that, by the same token, the spin asymmetry in the recoil regime should increase with atomic number (Keller *et al.* 1996*b*). A very recent experiment by Sauter *et al.* (1998*b*) confirmed this prediction. However, a close inspection of the theoretical data (paper II) shows that this dependence is only seen for forward emission of both electrons, whereas for backward emission, the asymmetry pattern changes completely between silver and gold targets. A preliminary analysis (see paper II) indicates that the transverse interaction between the active electrons also influences the measured asymmetries. However, it must be concluded that at present, the details of these asymmetries are not understood.

#### (4c) Fine Structure Effect

The fine structure effect first proposed by Hanne (Hanne 1992; Jones *et al.* 1994) is a delicate application of exchange scattering to analyse the total angular momentum state produced in electron inelastic scattering on a closed *p* level. It allows a spin asymmetry to be observed (i.e. the expectation value of the spin projection to be measured) even if only the projectile electrons are polarised, and no final state spin is observed. The idea is as follows: it is well known that electron impact excitation or ionisation of a closed *p* level leaves the residual

ion in a state with unevenly populated  $m_j$  levels in the natural frame, i.e. with an orientation. If the total angular momentum of the ion is known, i.e. if the fine structure splitting is energetically resolved, this orientation must be reflected in the population of the  $m_j$  levels of the ejected electron due to angular momentum conservation. This orientation includes a nonzero spin expectation value of the ejected electron, which can be probed by exchange scattering with electrons polarised in the natural frame (transverse polarisation): since direct and exchange amplitudes interfere in the triplet channel, but not in the singlet one, a spin asymmetry results.

The (e, 2e) fine structure effect has been investigated in detail for the case of the  $5p$  levels of xenon (Guo *et al.* 1996; Hanne 1996; Dorn *et al.* 1997; Mette *et al.* 1998). It was found that certain algebraic relations between the results for  $p_{1/2}$  and  $p_{3/2}$  levels, expected from the formal representation of the argument indicated above, were only qualitatively satisfied. Moreover, the DWBA description of these experiments was found to be only moderately successful (Dorn *et al.* 1997). To explain these observations, it has been argued that many-body effects have a significant influence on these outer shell TDCS and asymmetries (Madison *et al.* 1998). This would indicate that the (e, 2e) fine structure effect on outer shell electrons is much more complex than indicated by the argument given above.

It is therefore of considerable interest to study this phenomenon in a situation where at least the TDCS can be reasonably well understood. Thus, Besch *et al.* (1998) have considered the spin asymmetry for ionisation of the  $2p_{3/2}$  state of uranium. They observed large values of the asymmetry function in the binary collision region (Fig. 4), that would be difficult to explain in terms of continuum spin-orbit coupling. Indeed, a companion experiment using similar kinematics for the case of the  $K$  shell of silver (see Section 3) showed only very small

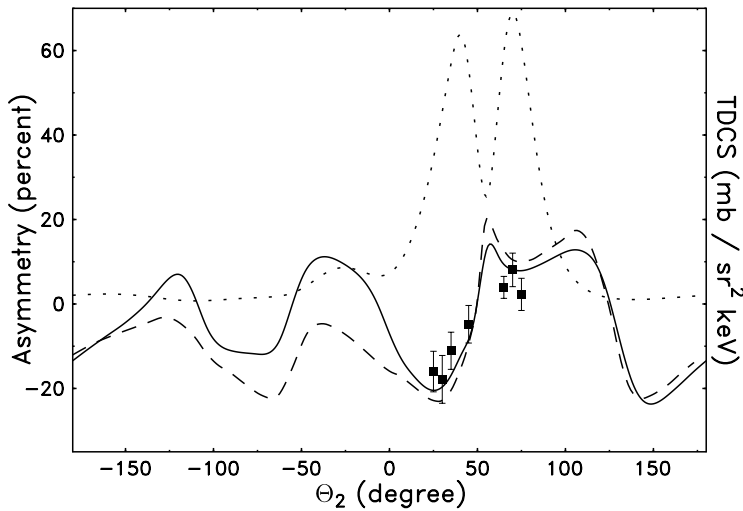


**Fig. 4.** Experimental and rDWBA results for spin asymmetries and TDCS. Electron impact ionisation of uranium  $2p_{3/2}$  shell by transversely polarised electrons is for  $T_0 = 300$  keV,  $T_1 = 210$  keV and  $\theta_1 = -24.8^\circ$ . Symbols: experimental spin asymmetry (Besch *et al.* 1998), full curve: calculated asymmetry, dashed curve: asymmetry calculated from  $S^{\text{long}}$  only, and dotted curve: calculated TDCS.

asymmetries (Besch *et al.* 1998). Of course, one might argue with reference to the comparison of TDCS in Fig. 3, that the strong nuclear field within the uranium atom could lead to an increase in the asymmetry. However, rDWBA calculations show that even for the case of ionisation of the uranium  $K$  shell, no such large asymmetry values in the binary regime occur. Moreover, the asymmetries in the binary region calculated for  $p$  states turn out to be essentially independent of the model used for the scattering wave functions in the Møller two-particle matrix element (Keller *et al.* 1996*b*). Finally, as shown in Fig. 4, neglecting the transverse photon exchange contribution to the asymmetry has little effect in the binary regime, in contrast to the results of paper II for the recoil regime mentioned above. In view of the good agreement between the measured asymmetries and the rDWBA results, it can therefore be concluded that this experiment has measured the fine structure effect in a rather ‘pure’ form.

## 5. Summary and Outlook

The various features of (e, 2e) TDCS for different target systems observed in experiments in coplanar asymmetric geometry can be explained in terms of the mechanisms included in the rDWBA model, namely Mott scattering of the active electrons in the field of the spectator ion, and interference of the amplitudes for ionisation by longitudinal and transverse single photon exchange. While the importance of the former mechanism increases strongly with target atomic numbers, the latter effect is relevant for all target systems, in particular for emission of both electrons into the same quadrant.

In marked contrast, only a rudimentary interpretation of observed and calculated spin asymmetries for ionisation by transversely polarised electrons is currently available. Recent experimental and theoretical results indicate that even the observed  $K$ -shell asymmetries are the result of a delicate interplay of different relativistic effects. At least, the main mechanisms, namely continuum spin-orbit coupling and (for  $p$  states) the Hanne fine structure effect, have unambiguously been identified.

Future studies of the inner shell ionisation TDCS will have to concentrate on a better understanding of the strong field effects in the recoil regime. In fact, little is known about the systematics of the recoil peak even in the nonrelativistic energy regime. In this context, experimental (e, 2e) data for ionisation of the  $1s$  electrons at impact energies of a few keV (e.g. for neon, aluminum or argon) would be extremely helpful. On the other hand, a deeper understanding of the spin asymmetries at present would seem to require mainly a theoretical effort. In particular, the symmetry properties of the relativistic scattering amplitudes need to be studied in more detail.

## Acknowledgments

Many of the results discussed in this work, and many more that I have not explicitly mentioned here, have been obtained in close collaboration with numerous colleagues from both experiment and theory. It is a pleasure to take this opportunity to express my gratitude to all of them for the most enjoyable experience of making a joint effort to understand the relativistic (e, 2e) process.

Specifically, I would like to emphasise the contributions of, and acknowledge fruitful discussions with, L. U. Ancarani, H. Ast, K.-H. Besch, B. Joulakian, T. Kull, H.-Th. Prinz, M. Sauter, C. D. Schröter, H. R. J. Walters and C. T. Whelan. I am most grateful to W. Nakel, who has been the prime source of inspiration for all the work in this field, for sharing his deep insights into the physics of relativistic electrons, and for his constant encouragement. However, my special thanks, not only for his important scientific contributions to this joint effort, but even more for his continuous support and good advice, go to my teacher, R. M. Dreizler.

## References

- Ast, H., Keller, S., Whelan, C. T., Walters, H. R. J., and Dreizler, R. M. (1994). *Phys. Rev. A* **50**, R1.
- Ast, H., Keller, S., Dreizler, R. M., Whelan, C. T., Ancarani, L. U., and Walters, H. R. J. (1996). *J. Phys. B* **29**, L585.
- Besch, K.-H., Sauter, M., and Nakel, W. (1997). *J. Phys. B* **30**, L73.
- Besch, K.-H., Sauter, M., and Nakel, W. (1998). *Phys. Rev. A* **58**, R2638.
- Bethe, H. (1933). *Z. Phys.* **76**, 293.
- Bonfert, J., Graf, H., and Nakel, W. (1991). *J. Phys. B* **24**, 1423.
- Briggs, J. S. (1986). *J. Phys. B* **19**, 2703.
- Butler, M. N., Chu, M.-C., Koonin, S. E., and Piecarewicz, J. (1988). *Phys. Rev. A* **37**, 2274.
- Dorn, A., Elliott, E., Guo, X., Hurn, J., Lower, J., Mazevet, S., McCarthy, I. E., Shen, Y., and Weigold, E. (1997). *J. Phys. B* **30**, 4097.
- Dreizler, R. M., Ast, H., Keller, S., Whelan, C. T., Ancarani, L. U., and Walters, H. R. J. (1997). *J. Phys. B* **30**, L77.
- Fontes, C. J., Sampson, D. H., and Zhang, H. L. (1995). *Phys. Rev. A* **51**, R12.
- Guo, X., Hurn, J. M., Lower, J., Mazevet, S., Shen, Y., Weigold, E., Granitza, B., and McCarthy, I. E. (1996). *Phys. Rev. Lett.* **76**, 1228.
- Hanne, G. F. (1992). Abstracts of Contributed Papers, ICPEAC XVII (Eds W. R. MacGillivray *et al.*), p. 199 (Hilger: Bristol).
- Hanne, G. F. (1996). *Can. J. Phys.* **74**, 811.
- Itzykson, C., and Zuber, J. B. (1980). ‘Quantum Field Theory’ (McGraw-Hill: New York).
- Jones, S., Madison, D. H., and Hanne, G. F. (1994). *Phys. Rev. Lett.* **72**, 2554.
- Keller, S. (1998). Habilitation thesis, University of Frankfurt, unpublished.
- Keller, S., and Dreizler, R. M. (1998). *Phys. Rev. A* **57**, 3652.
- Keller, S., Whelan, C. T., Ast, H., Walters, H. R. J., and Dreizler, R. M. (1994). *Phys. Rev. A* **50**, 3865.
- Keller, S., Dreizler, R. M., Ancarani, L. U., Walters, H. R. J., Ast, H., and Whelan, C. T. (1996a). *Z. Phys. D* **37**, 191.
- Keller, S., Dreizler, R. M., Ast, H., Whelan, C. T., and Walters, H. R. J. (1996b). *Phys. Rev. A* **53**, 2295.
- Keller, S., Dreizler, R. M., Ancarani, L. U., Ast, H., Walters, H. R. J., and Whelan, C. T. (1999). *Phys. Rev. A*, **59**, 1284.
- Kessler, J. (1985). ‘Polarised Electrons’, 2nd edn (Springer: Berlin).
- Kull, T., Nakel, W., and Schröter, C. D. (1997). *J. Phys. B* **30**, L815.
- Madison, D. H., Kravtsov, V. D., and Mazevet, S. (1998). *J. Phys. B* **31**, L17.
- Mette, C., Simon, T., Herting, C., Hanne, G. F., and Madison, D. H. (1998). *J. Phys. B* **31**, 4689.
- Moisewitsch, B. L. (1980). *Prog. At. Mol. Phys.* **16**, 281.
- Møller, C. (1931). *Z. Phys.* **70**, 786.
- Moore, D. J., and Reed, K. J. (1995). *Phys. Rev. A* **51**, R9.
- Pindzola, M. S., and Buie, M. J. (1988). *Phys. Rev. A* **37**, 3232.
- Pindzola, M. S., Moore, D. L., and Griffin, D. C. (1989). *Phys. Rev. A* **40**, 4941.
- Prinz, H.-Th., and Keller, S. (1996). *J. Phys. B* **29**, L651.

- Prinz, H.-Th., Besch, K.-H., and Nakel, W. (1995). *Phys. Rev. Lett.* **74**, 243.
- Sauter, M., Keller, N., and Nakel, W. (1998*a*). *J. Phys. B* **31**, L947.
- Sauter, M., Ott, H., and Nakel, W. (1998*b*). *J. Phys. B* **31**, L967.
- Whelan, C. T., Ast, H., Walters, H. R. J., Keller, S., and Dreizler, R. M. (1996). *Phys. Rev. A* **53**, 3262.
- Zhang, X., Whelan, C. T., Walters, H. R. J., Allan, R. J., Bickert, P., Hink, W., and Schönberger, S. (1992). *J. Phys. B* **25**, 4325.

Manuscript received 2 October 1998, accepted 7 January 1999